89-2-40
高工研図書室

INSTITUTE OF THEORETICAL
AND EXPERIMENTAL PHYSICS

173—88

V.S.Popov, V.D.Mur,
A.V.Sergeev, A.V.Scheblykin

SCALING FOR STARK EFFECT IN RYDBERG ATOMS

Moscow — ATOMINFORM — 1988

УДК 530.145 М-16

SCALING FOR STARK EFFECT IN RYDBERG ATOMS: Preprint ITEP 88-173/ V.S.Popov, V.D.Mur*, A.V.Sergeev,** A.V.Scheblykin - M.:ATOMINFORM, 1988 - 44p.

Equations determining the shifts and widths of the Rydberg states in a strong electric field (for an arbitrary atom) have been obtained, as well as scaling relations for nearthreshold Stark resonances with $n_1 \approx n \gg 1$, n_2 and $m \sim 1$ (n_1, n_2, m are parabolic quantum numbers). These relations are in agreement with experiment. The effect of barrier penetrability is taken into account.

Fig. - 7, ref. - 20

© Институт теоретической и экспериментальной физики, 1988

*) Moscow engineering physical institute

**) Vavilov state optical institute.

1. In the last few years the research of highly excited, or the Rydberg states of atoms and molecules attracts a considerable interest. The resonances in atomic photoionization cross sections in the presence of electric field $\mathcal{E}$ were experimentally discovered, with $n = 15 \div 40$ and energy $B \approx 0$ [1-5]. Numerical calculations carried out for a hydrogen atom [6,7] show that positions and widths of resonances coincide with complex energies, $E^{(n_1, n_2, m)} = E_r - i\Gamma/2$, of the Stark quasistationary states [1]. This makes it possible to experimentally verify the theory of the Stark effect in strong fields.

We have developed the analytical theory of the Rydberg states in an external electric field applicable to any atom, see eqs. (2)-(4) below. Using 1/n-expansion we obtained scaling relations for nearthreshold resonances which agree with the experiment. These relations can be used for identification of quantum numbers of resonances.

If not specified, we use atomic units, $\hbar = m_e = e = 1$; $n = n_1 + n_2 + m + 1$ is the principal quantum number, n_1, n_2, m are parabolic quantum numbers ($m \geq 0$).

2. Basic equations. When calculating the energies of (n_1, n_2, m) states with $n \gg 1$ and $m \ll n$, we use the WKB quantization conditions (including corrections of the order $\hbar^2$ [8]), approximate separation of variables in the region $r > r_a$ [2] and "hidden" symmetry of the Coulomb field [9]. If the separation constants are $\beta_{1,2}$ while the reduced energy and electric field are ϵ and F,

$$\epsilon = 2n^2 E^{(n_1 n_2 m)} = \epsilon' - i\epsilon'', \quad F = n^4 \mathcal{E}, \qquad (1)$$

then we get the equations

$$\beta_1 (-\epsilon)^{-3/2} f(z_1) - \frac{F}{8n^2} (-\epsilon)^{-3/2} [g(z_1) - m^2 h(z_1)] = \nu_1 ,$$

$$\beta_2 (-\epsilon)^{-3/2} f(z_2) + \frac{F}{8n^2} (-\epsilon)^{-3/2} [g(z_2) - m^2 h(z_2)] = \nu_2 , \qquad (2)$$

$$\beta_1 + \beta_2 = 1$$

(their derivation will be given elsewhere). Here

$$z_i = (-1)^i \beta_i F/\epsilon^2, \quad \nu_i = \left(1 - \frac{\delta}{n}\right)\left(n_i + \frac{m+1}{2}\right)/n, \quad i = 1, 2,$$

$\delta = \delta(n_1 n_2 m)$ is expressed through quantum defects μ_ℓ [10] for a free atom,

$$\delta(n_1 n_2 m) = \frac{1}{n} \sum_{\ell=m}^{n-1} (2\ell+1) \left(C^{JM}_{J, M-m; \ell m}\right)^2 \mu_\ell , \qquad (3)$$

J = (n-1)/2, M = $(n_1 - n_2 + m)/2$ and f , g , h are expressed through hypergeometric function F(z) ≡ ${}_2F_1(\ldots; z)$:

$$f(z) = F\left(\tfrac{1}{4}, \tfrac{3}{4}; 2; z\right),$$

$$g(z) = \tfrac{1}{3} F\left(\tfrac{3}{4}, \tfrac{5}{4}; 2; z\right) + \tfrac{2}{3} F\left(\tfrac{3}{4}, \tfrac{5}{4}; 1; z\right), \qquad (4)$$

$$h(z) = F\left(\tfrac{3}{4}, \tfrac{5}{4}; 2; z\right).$$

The quantum defect δ in a parabolic basis is due to the difference of atomic field from the Coulomb one, $V_C(z) = -1/z$,

at $t \lesssim t_a$. The appearance of the Clebsh-Gordan coefficients in eq.(3) is accounted for by the hidden symmetry group of a hydrogen atom SO(4) ≈ SO(3) SO(3) while $\vec{L} = \vec{J}_1 + \vec{J}_2$ where $\vec{L}$ is angular momentum and $\vec{J}_i$ are generators of one of the SO(3) subgroups.

Since μ_ℓ sharply decreases with ℓ growing[10], only a few terms remain in the sum (3) . Asymptotically $\delta(n_1 n_2 m) \to \frac{1}{n} \to 0$ as $n \to \infty$ but they are not small enough at n = 20 ÷ 30 (see Table 1). Note that at n fixed $\delta(n_1 n_2 m)$ are maximum for the n_2=m=0 states, when

$$\delta(n-1,0,0) = \frac{1}{n}\left[\mu_0 + \sum_{\ell=1}^{n-1}(2\ell+1)\frac{(n-1)\dots(n-\ell)}{(n+1)\dots(n+\ell)}\mu_\ell\right] \qquad (3')$$

With n_2 increasing and especially with increasing of magnetic quantum number m, $\delta(n_1 n_2 m)$ rapidly decrease (see Table 1), therefore the spectrum of these states approaches that of hydrogen.

The corrections disregarded in eqs.(2) do not exceed n^{-4} , thus the accuracy of eqs.(2) is high enough for the Rydberg states. At $\mathcal{E} \to 0$ the solution of (2) agrees with the perturbation series up to terms of the order $\mathcal{E}^3$ (see Appendix A). However, eqs.(2) allow one to consider the case of strong fields as well, up to the $\mathcal{E}$ values comparable to the field in an electron orbit, $n^4\mathcal{E} \sim 1$.

Though eqs.(2) can be solved numerically, at n >> 1 it would be natural to use 1/n-expansion. For states with $n_1 \sim n \gg 1$ and $n_2, m \sim 1$ we get

$$\varepsilon^{(n_1 n_2 m)} = \varepsilon_0 + \frac{\rho}{n}\varepsilon_1 + \frac{1}{n^2}(\rho^2\varepsilon_2 + \xi_2 + m^2\eta_2) + O\left(\frac{1}{n^3}\right) \qquad (5)$$

$P = 2n_2 + m + 1$. Within $n \to \infty$ the system (2) is reduced to a single equation

$$(-\varepsilon)^{3/2} = F\left(\tfrac{1}{4}, \tfrac{3}{4}; 2; -16F/\varepsilon^2\right) \qquad (6)$$

whose solution we denote by $\varepsilon_\alpha \equiv \varepsilon_0(F)$. It can be easily shown that ε_α monotonously grows with P, crosses $\varepsilon = 0$ at $P = P_* = 0.3834$ and remains real at all F, $0 < F < \infty$. Since $P = P_*$ is not a singularity for the function $\varepsilon_\alpha(F)$ it can be expanded over integer powers of $f = (F-F_*)/F_*$,

$$\varepsilon_\alpha(F) = \alpha_1 f + \alpha_2 f^2 + \alpha_3 f^3 + \ldots \qquad (7)$$

($\alpha_1 = 0.9034$, $\alpha_2 = -0.0674$, $\alpha_3 = 0.0173$, $\alpha_4 = -0.0063$, etc). At the same time the function $\gamma_\alpha(F)$ has a square root singularity at $F = F_*$, see eq.(B.6). A sharp decrease of coefficients α_k starting from k=2 accounts for approximate linearity of the graph ε_α in Figs.3 and 4. The properties of the functions $\varepsilon_\alpha(F)$ and $\gamma_\alpha(F)$ are discussed in Appendix B, see also Table 2.

The next terms of 1/n-expansion acquire an imaginary part at $P > P_*$, the terms of 1/n and $1/n^2$ order in (5) being expressed through $\varepsilon_\alpha(F)$ and its derivatives, see Appendix B. Using the above, we come to the scaling relations:

$$E_t^{(n,n_2,m)} = \frac{1}{2\tilde{n}^2}\varepsilon_\alpha(\tilde{n}^4\mathcal{E}), \quad \Gamma^{(n,n_2,m)} = \frac{\rho n_*}{n\tilde{n}^3}\gamma_\alpha(\tilde{n}^4\mathcal{E}), \qquad (8)$$

where $n_* = n - \delta$, $\tilde{n} = n_1 + \frac{m+1}{2} - \delta$ $\left(n_* - \tilde{n} = \rho/2\right)$

$$\gamma_{\alpha\ell}(F) = \theta(F-F_*)\left(F\frac{d}{dF}-1\right)\varepsilon_{\alpha\ell}^{3/2}$$

and $E > 0$. In the subthreshold region $E < 0$ we have instead of (8):

$$E_\tau^{(n_1 n_2 m)} = \frac{1}{2\tilde{n}^2}\left[\varepsilon_{\alpha\ell}(\tilde{n}^4\mathcal{E}) + \gamma\left((\tilde{n}n_*)^2\mathcal{E}\right) - (\tilde{n}/n_*)^2\gamma\left(n_*^4\mathcal{E}\right)\right], \quad \gamma(F) = \left[-\varepsilon_{\alpha\ell}(F)\right]^{3/2} \tag{9}$$

Note that eqs.(6) and (7) contain a single universal function $\varepsilon_{\alpha\ell}(F)$ which is determined by eq.(6). The values of $\varepsilon_{\alpha\ell}$ and $\gamma_{\alpha\ell}$ are given in Table 2 and their expansions near $F=F_*$ are given in Appendix B. The scaling relations have relative accuracy $1/n^2$.

3. Eqs.(8) involve some relationships which have been earlier observed empirically basing on numerical calculations. We note here the following:

a)The Stark level $(n_1 n_2 m)$ intersection of energy $E=0$ (ionization limit with no external field, $\mathcal{E} = 0$) corresponds to the following value of the principal quantum number n,

$$n = n^{(0)} = k\mathcal{E}^{-1/4} + n_2 + \frac{m+1}{2} + \delta(n_1 n_2 m), \tag{10}$$

where $k = (2\gamma/9\varkappa)^{1/2}$ = 0.787 in atomic units and k=37.5 if electric field $\mathcal{E}$ is measured in kV/cm (here γ is the numerical constant introduced in B(4)). As usual, series of resonances at fixed $\mathcal{E}$, n_2 and m are experimentally observed (with $n_1 \sim n >> 1$, while n_2 , $m \sim 1$).

Formula (10) is just the case. The corresponding value of quantum number n_1 is $n_1^{(0)} = k\mathcal{E}^{-1/4} - \frac{m+1}{2} + \delta$.

6) Consider the slope of the $(n_1 n_2 m)$ level at E=0. In reduced variables $\mathcal{E}$, F

$$\left.\frac{d\mathcal{E}'_{n_1 n_2 m}}{dF}\right|_{\mathcal{E}=0} = \frac{3\pi}{4}\left\{1 - \frac{n_2 + \frac{m+1}{2} + \delta}{n} + O\left(\frac{1}{n^2}\right)\right\} \qquad (11)$$

With increase of quantum numbers n_2 and m the slope decreases which completely agrees with numerical calculations (see Fig.1 in [7]).

c) Numerical calculations show that for states (n-2,1,0) and (n-3,0,2) in a hydrogen atom the reduced energies $\mathcal{E}'_{n_1 n_2 m} = 2n^2 E_t^{(n_1 n_2 m)}$ are very close to each other in the region $E \approx 0$. For example, in Fig.1 in [7] the curves for states (23,1,0) and (22,0,2) coincide up to the accuracy of the figure. Note that the above states have the same value $p = 2n_2 + m + 1 = 3$. n=25 and,

The explanation of the fact follows directly from eq.(8). At fixed value of $\mathcal{E}$ the position and width of the Stark states with the same p and $\tilde{n} = n - P/2$:

(n-2,1,0) and (n-3,0,2), p = 3;

(n-3,1,1) and (n-4,0,3), p = 4;

(n-3,2,0), (n-4,1,2) and (n-5,0,4), p = 5,

differ only in terms $\sim 1/n^2$, etc. On the other hand, for states (n-m-1,0) with m = 0,1,2... << n, for example, we have P = m+1, $\tilde{n} = n-(m+1)/2$. Thus, the values of $\mathcal{E}'$ and $\mathcal{E}''$ for them are different already in terms $\sim 1/n$.

d) Since $\tilde{n}$ is n_2- independent, for states with given quan-

tum numbers n_2 and m the energy $E^{(n_1 n_2 m)}$ must be close and their widths proportional to p (at $E > 0$). This conclusion is supported by numerical calculations (see Fig.3 in [7]). When going over into $E > 0$ region the shifts between the energies of $(n_1,0,0)$ and $(n_1,1,0)$ states rapidly decrease, while

$$\Gamma^{(n_1,0,0)} : \Gamma^{(n_1,1,0)} : \Gamma^{(n_1,2,0)} \approx 1 : 3 : 5 \qquad (12)$$

e) The resonance peak width at $E > 0$ rapidly increases with the energy increase. From condition $\Gamma = \Delta E$ one can estimate the value of $n = n_c$ (at fixed $\mathcal{E}$), for which the neighbouring Stark resonances become overlapped and the structure in photoionization cross sections disappears.

In the lower order in 1/n, one can readily get, using scaling (8) and linear approximation: $\varepsilon_{cl}(F) \approx \alpha_1 f$,

$$n_c = k_c \mathcal{E}^{-1/4} + n_2 + \frac{m+1}{2} + \delta \qquad (10')$$

where $k_c = k(1+f_c)^{1/4}$, k is defined in (10) and f_c is the root of equation $f\left[(1+f/3)/(1+f/2)\right]^2 = 1.97\ p^{-2}$ (in particular, $f_c = 3.09$, 0.574 and 0.235 at p = 1, 2 and 3).

Hence it is easy to estimate the number of resonance peaks Δn which can be observed in the abovethreshold region: $\Delta n \approx k_1 \mathcal{E}^{-1/4}$, where $k_1 = 0.787\ ([1+f_c]^{1/4} - 1)$. For example, at $\mathcal{E} = 8.0$ kV/cm we get $\Delta n \approx 9$ for $(n_1,0,0)$ states and $\Delta n \approx 1$ for $(n_1,1,0)$ states. These values are in a qualitative agreement with numerical calculations[7].

4. The classical ionization threshold F_* . Let us start with the states (0,0,n-1), which within $n \to \infty$ correspond to the circular orbits of an electron in the plane normal to the field $\vec{\mathcal{E}}$. Using scaling transformation $\vec{\varepsilon} \to n^2 \vec{\varepsilon}$ in the Schrödinger equation one can easily see that n is analogous to mass. In $1/n$-expansion $\varepsilon_0 = U_{min}$, that corresponds to the classical particle at rest at the minimum of effective potential U(r). The next terms $\varepsilon_1, \varepsilon_2, \ldots$ correspond to the zero energy fluctuations around the classical equilibrium point and to anharmonism corrections.

Employing equlibrium conditions of electron in the circular orbit, we get [11,12]

$$\varepsilon_0 = -(1+3\tau^2)(1-\tau^2)^2, \quad F = \tau(1-\tau^2)^4, \qquad (13)$$

where $\tau = \tau(F) \to 0$ at $F \to 0$. Corrections ε_1 and ε_2 are also determined analytically while the next coefficients of 1/n expansion ε_k are found by recurrence ratios. [13]

It is seen from (13) that at $\tau = 1/3$ or $F = F_* = 0.2081$ two solutions collide. At $F > F_*$ the minimum in the effective potential $U_2(\eta)$ disappears and the classical equilibrium point moves onto complex plane. This allows one to describe, within the 1/n-expansion, not only the Stark shift but also the width $\Gamma^{(n_1 n_2 m)}$ of quasistationary states (cf. a similar situation with the Yukawa and Hulthén potentials [14]).

It is natural to call F_* the classical ionization threshold In general case F_* depends, whithin $n \to \infty$, only on ratios $\mu = m/n$ and $\varkappa_i = n_i/n$ (with $\varkappa_1 + \varkappa_2 + \mu = 1$). To calculate

F_* for the case $\mu = 0$ one should put $Z_2 = 1$ in eqs.(2) (for more details see ref.[11]. We calculate F_* for all states where one of the numbers $\varkappa_1$, $\varkappa_2$ or μ is 0. The results are presented in Fig.1. The values of F_* for arbitrary states (n_1, m_2, m) are within the curvilinear triangle bound by the curves in Fig.1. (see also ref.[15] and Table 4.

Until $F < F_*$, the coefficients $\varepsilon_k(F)$ in expansion (4) are real and ionization of atomic states by electric field $\mathcal{E}$ is of a tunnel character. At $F > F_*$ the barrier in the effective potential $U_2(\xi)$ disappears and the width $\Gamma^{(n_1 n_2 m)}$ is no longer exponentially small. Therefore the values of F_* is of some interest for the theory of atom ionization by electric field, particularly for the case of the Rydberg states.

5. Comparison with experiment. Let us begin with subthreshold resonances in a hydrogen atom. The data on their positions and widths have been published recently [5] . In Table 3 two series of such resonances are considered: with $n_1 \gg n_2$ and $n_1 \leq n_2$ (in these cases m=0 which is explained by atom excitation by lazer light with π -polarization). We have used two calculation methods: summation of divergent perturbation series with the help of Hermite-Padé approximant (HPA) and 1/n-expansion which is reduced to the solution of system (2). As is seen from Table 3, the agreement between theory and experiment is good enough(4) .

In Fig.1 the energies of Stark resonances in a hydrogen atom are compared with experimental spectra of photoionization [4]. The values of $E_z^{(n_1 n_2 m)}$ were calculated by HPA and are depicted by solid lines, a bundle of lines with the given $(n_1 n_2 m)$

characterizing the width of the level $\Gamma^{(n_1 n_2 m)}$. The experimental spectra are taken from [4] and correspond to $\mathcal{E}$ = = 6.5, 8.0, 14.3 and 16.9 kV/cm (from left to right in Fig.1).

In Fig.2 scaling (8) for $E_r(n_1,n_2m)$ is verified. The experimental points: O - the states $(n_1,0,0)$ in a hydrogen atom[4] at $\mathcal{E}$ = 6.5 and 8.0 kV/cm; □ - series $(n_1,0,1)$ and $(n_1,1,0)$ in a hydrogen atom[4]; + - the data for Rb[1] at $\mathcal{E}$ = 2.189 kV/cm (the left four points) and also $\mathcal{E}$ = 4.335 and 6.416 kV/cm, *-states $(n_1,0,0)$ for Na[2,3], $\mathcal{E}$ = 2.15 and 4.46 kV/cm.

One important point should be noted which is essential when treating the spectra for Rb[1]. Experimental points fit the universal curve $\varepsilon_{el}(\tilde{F})$ in Fig.2 only when the value of $\delta(n-1,0,0)$ is taken into account and the values of n given in ref.[1] are increased by 1. Otherwise we get points Δ in Fig.3a the distance of which from the curve $\varepsilon_{el}(\tilde{F})$ is far off the experimental errors. Such a change of n is confirmed by comparison of our calculations with experimental photoionization spectra near E = 0. Thus, according to eq.(10), $n^{(0)}$=31.8 at $\mathcal{E}$ = 2.189 kV/cm. On the other hand, as is seen from Fig.6, the ionization limit $E = 0$ (λ = 2967.5Å) corresponds to n = = 30.7 ≈ $n^{(0)}$ - 1. The error in ref.[1] results, apparently, from the use of PT (of the 4-th order in $\mathcal{E}$) in identifying the peaks of subbarrier region for a hydrogen atom while in the Rb case the quantum defect correction $\delta(n_1 n_2 m)$ is essential and should be taken into account.

Fig.4 illustrates the validity of eq.(9) for the subthreshold Stark resonances. Experimental points are taken from refs. [2,4,5] and are recalculated in the following way:

$$\Delta_{n_1 n_2 m} = 2\tilde{n}^2 E_r^{(n_1 n_2 m)} + \left(\frac{\tilde{n}}{n_*}\right)^2 \eta(n_*^4 \mathcal{E}) - \eta((\tilde{n} n_*)^2 \mathcal{E}) \qquad (14)$$

If eq.(9) would be exact, then the corresponding points depending on variable $\tilde{F} = \tilde{n}^4 \mathcal{E}$ had to fit the universal curve $\mathcal{E}_{cl}(\tilde{F})$ up to $\sim 1/n^2$. As is seen from Fig.4, this is just the case. The notations are the following:

○ - states $(n_1, n_2, 0)$ in a hydrogen atom[4] at $\mathcal{E} = 16.8$ kV/cm. Here $10 \leq n_1 \leq 17$ and $4 \geq n_2 \geq 0$.

● - states $(n_1, n_2, 0$- in hydrogen[4] at $\mathcal{E} = 8.0$ kV/cm; $15 \leq n_1 \leq 21$, $n_2 = 0$ and 1.

\+ - states $(n_1, 0, 0)$ in a Rb atom[1]; $\mathcal{E} = 2.189$ kV/cm, $n_1 = 19 \div 24$ (left to right).

✳ - states $(n_1, 0, 0)$ in Na[2]; $\mathcal{E} = 3.59$ kV/cm and $n_1 = 23 \div 26$.

The quantum numbers n_1, n_2 of some states are shown in Fig.4. Note that the points corresponding to fixed n_1 and $n_2 = 0 \div 4$, coincide within the accuracy of the figure. Thus, relation (9) is experimentally confirmed.

As for the width of resonances, at $F > 0.45$ the experimental points fit rather well the universal scaling curve according to eq.(8) but at smaller F there is a deviation from scaling (see Fig.5 where points ○, □ and ▽ correspond to

p=1, 2 and 3). We shall examine the reason in the next section.

6. Barrier penetreability correction. So far when calculating the position and width of resonances we have proceeded from eqs.(2) obtained from quasiclassical quantization conditions. Here the width of the level is identical zero up to $F < F_*$ though in fact it is not zero because of the finite barrier penetreability in the potential $U_2(\eta)$. It can be shown that the account of the effect results in a substitution

$$\nu_2 \to \nu_2 - \frac{1}{2\pi n}\varphi(a) \qquad (15)$$

in eqs.(2). Here

$$a = \frac{1}{\pi}\int_{\eta_1}^{\eta_2}|p_\eta|d\eta\ ,\quad |p_\eta| = \left(\frac{m^2}{4\eta^2} - \frac{\beta_2}{\eta} - \frac{\mathcal{E}}{4}\eta - \frac{E}{2}\right)^{1/2} \qquad (16)$$

$(\eta_1 < \eta < \eta_2$ is a subbarrier region) and, in 1/n-approximation,

$$\varphi(a) \equiv \varphi_1 = \frac{1}{2i}\ln\frac{\Gamma\left(\frac{1}{2}+ia\right)}{\Gamma\left(\frac{1}{2}-ia\right)\left(1+e^{-2\pi a}\right)} - a\ln a + a, \qquad (17)$$

while in $1/n^2$-approximation, i.e. when the terms $F/8n^2$ in eq. (2) are taken into account,

$$\varphi(a) \equiv \varphi_2 = \varphi_1(a) - \frac{1}{24a} \qquad (17')$$

(The derivation of the equations will be published elsewhere). At $\mathcal{E} \to 0$ we get

$$a = \frac{n}{3\pi}\left\{F^{-1} + \frac{3\beta}{2n}\ln F + O(1)\right\} \to \infty \qquad (18)$$

$$\varphi_2(a) = \frac{1}{2880\, a^3} + O\left(\frac{1}{a^5}\right) + \frac{i}{2} e^{-2\pi a} + \cdots \qquad (19)$$

($|a| \to \infty$, $\mathrm{Re}\, a > 0$). Therefore eqs.(2) and (15) go over, up to terms $\sim n^{-4}$, into usual quasiclassical quantization conditions while the account of pure imaginary term in (19) determines the width of the level:

$$\Gamma^{(n,n_2 m)} = \frac{1}{2\pi n^3} e^{-2\pi a} = \tilde{A}_{n,n_2 m} F^{-p} e^{-\frac{2n}{3F}},$$

$$\tilde{A}_{n,n_2 m} = \frac{e^{3n}}{2\pi n^3} \left(\frac{4n}{e^2}\right)^p \frac{1}{(n_2+\frac{1}{2})^{n_2+\frac{1}{2}}} \cdot \frac{1}{(n_2+m+\frac{1}{2})^{n_2+m+\frac{1}{2}}}, \qquad (20)$$

$p = 2n_2 + m + 1$. Note that the exact threshold behaviour of width $\Gamma^{(n,n_2 m)}$ at $F \to 0$ functionally has the form (20) but the preexponential factor is[17,18]

$$A_{n,n_2 m} = \frac{e^{3n}}{n^3} \left(\frac{4n}{e^3}\right)^p \frac{1}{n_2!} \cdot \frac{1}{(n_2+m)!} \qquad (20')$$

Eqs.(20) and (20') differ only in substitution of factorials by the Stirling formula, namely,

$$\tilde{A}_{n,n_2 m} / A_{n,n_2 m} = \omega(n_2)\,\omega(n_2+m), \qquad (21)$$

$$\omega(x) = \frac{x!}{\sqrt{2\pi}\left(\frac{x+\frac{1}{2}}{e}\right)^{x+\frac{1}{2}}} = \begin{cases} 0.930, & x = 0 \\ 0.973, & x = 1 \\ 1 - \frac{1}{24x} + \ldots, & x \gg 1 \end{cases}$$

Thus, in the region of weak fields the correction (15) allows one to find $\Gamma^{(n,r_2,m)}$ with high precision.

Note that at m=0 the integral (16) is calculated analytically [8] :

$$a = \frac{n(-\epsilon)^{1/2}}{2^{1/2}F}(1-z_2)f(1-z_2), \qquad (22)$$

where $z_2 = 16\beta_2 F/\epsilon^2$ and f(z) is defined in (4). The function $\varphi(a)$ entering eq.(15) has singularities (besides $a=0$) at

$$a = (n+\tfrac{1}{2})i \quad , \; n = 0,1,2, \ldots, \qquad (23)$$

which correspond to poles of the scattering ampliitude for a parabolic barrier. Indeed, the solution of the Schrödinger equation with $V(x) = -m\omega^2x^2/2$ can be expressed by the parabolic cylinder functions

$$\psi = \text{const}\; D_{-ia-1/2}\left(2^{1/2}e^{-i\pi/4}\xi\right) =$$

$$= \begin{cases} (-\xi)^{ia-1/2}e^{-i\xi^2/2} + A(-\xi)^{-ia-1/2}e^{i\xi^2/2}, & \xi \to -\infty \\ B\xi^{-ia-1/2}e^{i\xi^2/2}, & \xi \to +\infty, \end{cases}$$

where $x = (\hbar/m\omega)^{1/2}\xi$, $B = ie^{-\pi a}A$ and $a = -E/\hbar\omega$. Using the standard formulae for the asymptotics of $D_\nu(z)$ we get

$$A = -i\frac{(2\pi)^{1/2}2^{-ia}\exp(\pi a/2)}{\Gamma(\frac{1}{2}-ia)\left[1+\exp(-2\pi a)\right]} \qquad (24)$$

It is seen from (24) that the reflection amplitude A has poles at the points (23), the wave function in this case being

$$\psi_n \sim \xi^n \exp(i\xi^2/2), \quad \xi \to \pm\infty \qquad (25)$$

On the other hand, at $\alpha = -(n+\frac{1}{2})i$ the amplitude A is finite. The presence of poles of A at these points would contradict hermiticity of the hamiltonian as in this case the quadratically integrable wave functions would exist $(n \geq 0)$

$$\psi_n \sim \xi^{-(n+1)} \exp(i\xi^2/2), \quad \xi \to \pm\infty \qquad (25')$$

corresponding to the complex energy eigenvalues $E_n = i(n+\frac{1}{2})\hbar\omega$.

7. Numerical calculations. The system (2),(15) for m=0 was solved numerically (expression(22) for α was used). The results of calculations for (n-1 ,0,0) states with n=20 and 50 in a hydrogen atom are shown in Figs.6,7. The notations: curve 1 corresponds to the solution of eq.(2) neglecting the barrier penetr ability (i.e. $\nu_2 = 1 - \nu_1 = 1/2n$), curves 2 and 3 - with the penetr sbility taken into account, i.e. ν_2 according to (15). Besides, curves 1 and 2 correspond to 1/n-approximation (i.e. in eq.(2) the terms $F/8n^2$ were omitted) and curve 3 - to $1/n^2$-approximation. As is seen from the figures, the barrier penetreability is of principal importance at $F \lesssim F_*$. In the region $F > F_*$ curve 2 (and, particularly, 3) rapidly approaches the curve $\varepsilon_n''(F)$) which is calculated neglecting penetreability. Therefore it is possible to use here the simplest form of 1/n-expansion without barrier penetreabilit/y correction.

Thus, numerical solutions of system (2),(15) provide correct interpolation between the region of the weak field and the scaling region $F > F_*$. The validity of the results obtained can be also confirmed by comparing them with the values $\Gamma^{(n_1 n_2 m)}$ obtained by HPA. Thereby one can overcome the difficulty arised earlier [14] when describing quasistationary states within 1/n-expansion (in the region prior to collision of classical solutions where 1/n-expansion always resulted in the zero width of the level).

As for the barrier penetreability effect on the level position, it is small (see Table 5). It should be emphasized here that the account of barrier penetreability essentially stabilizes the calculated values of energies: the difference between 1/n and $1/n^2$ approximations for $\mathcal{E}_n' = Re\, \mathcal{E}^{(n-1,0,0)}$ is not more than 0.5%.

Let us compare the results of the calculations of widths $\Gamma^{(n_1 n_2 m)}(\mathcal{E})$ with the experimental data. Nowadays, the data published in [5] for states $(n_1, n_2, 0)$ in a hydrogen atom refer only to the subthreshold region. Note that resonance widths are not yet reliably determined (in particular, for asymmetric resonances two possible values of $\Gamma/2$ are given [5]). Theoretical estimates of $\Gamma^{(n_1 n_2 m)}(\mathcal{E})$ was made according to system (2) taking into account (15) in $1/n^2$-approximation. The results given in Table 3 show that as a whole there is an agreement between theory and experiment though the accuracy here is less than that obtained for the resonance positions.

8. Thus, the agreement between theory and experiment leaves no doubt as to the fact that the observed peaks in the photoionization cross sections correspond to the Stark quasistationary

states (both in the subthreshold region, $E < 0$, and at $E > 0$, while $\Gamma \lesssim \Delta E$). The application of 1/n-expansion possessing a high degree of accuracy for the Rydberg states made it possible to obtain scaling relations (8),(9) for the positions and widths of the Stark resonances for an arbitrary atom. Scaling relations agree well with experiment and can be used to identify quantum numbers $n_1 n_2 m$. When calculating the level widths in the region $F \lesssim F_*$ it is essential to introduce correction for the barrier penetreability in quasiclassical quantization rules.

Appendix A.

Equations (2) and PT

In the weak field region we get: $\varepsilon \to -1$ and $z_{1,2} \to 0$. Introducing variables $t_i = \beta_i (-\varepsilon)^{-1/2}$ let us rewrite eq. (2) in a form more convenient for iteration at $F \to 0$:

$$t_1 = \nu_1 \varphi(z_1) + \frac{F}{8\pi^2}(t_1+t_2)^3\left[\psi(z_1) - m^2 \chi(z_1)\right],$$
$$t_2 = \nu_2 \varphi(z_2) - \frac{F}{8\pi^2}(t_1+t_2)^3\left[\psi(z_2) - m^2 \chi(z_2)\right], \qquad (A.1)$$

where $z_i = (-1)^i \cdot 16\, F\, t_i (t_1 + t_2)^3$ for i=1 and 2,

$$\varphi = 1/f(z), \quad \psi = g(z)/f(z), \quad \chi = h(z)/f(z) \qquad (A.2)$$

and functions f, g and h are determined in (4), where

$$\varepsilon = -(t_1+t_2)^{-2}, \quad \beta_i = \frac{t_i}{t_1+t_2} \qquad (A.3)$$

Taking into account the expansions

$$f(z) = \sum_{k=0}^{\infty} \frac{(4k-1)!!}{k!\,(k+1)!}\left(\frac{z}{16}\right)^k = 1 + \frac{3}{32}z + \frac{35}{1024}z^2 + \dots,$$
$$g(z) = 1 + \frac{25}{32}z + \frac{735}{1024}z^2 + \dots, \qquad (A.4)$$
$$h(z) = 1 + \frac{15}{32}z + \frac{315}{1024}z^2 + \dots,$$

we find

$$\varphi = 1 - \frac{3}{32}z - \frac{13}{512}z^2 + \dots, \quad \psi = 1 + \frac{11}{16}z + \frac{317}{512}z^2 + \dots,$$

$$\chi = 1 + \frac{3}{8}z + \frac{61}{256}z^2 + \dots$$

at $z \to 0$. Now eqs.(A.1) can be easily solved by iterations. The initial approximation is $t_1^{(0)} = \nu_1$, $t_2^{(0)} = \nu_2$; then we get $t_1 = \nu_1 + \left(\frac{3}{2}\nu_1^2 - \frac{m^2-1}{8n^2}\right)F^2 + \dots$, $t_2 = \nu_2 - \left(\frac{3}{2}\nu_2^2 - \frac{m^2-1}{8n^2}\right)F^2 \dots$,

$$\epsilon = -1 + 3\alpha F^2 - \frac{1}{8}\left(17 - 3\alpha^2 - 9\mu^2 + 19\frac{1}{n^2}\right)F^4 + \dots \qquad (A.5)$$

$$\beta_2 = \frac{1+\alpha}{2} + \frac{1}{8}\left[3(1-\alpha^2) - \frac{m^2-1}{n^2}\right]F^2 +$$

$$+ \frac{\alpha}{16}\left(1 - \alpha^2 - 6\frac{m^2-1}{n^2}\right)F^4 + \dots \qquad (A.6)$$

Here $\nu_i = (n_i + \frac{m+1}{2})/n$, $\alpha = \nu_1 - \nu_2 = (n_1 - n_2)/n$, $\mu = m/n$; and the series for $\beta_2(F^2)$ is obtained by substituting $\nu_1 \rightleftarrows \nu_2$, $\alpha \to -\alpha$ and $F^2 \to -F^2$. The last expansions coincide up to F^2 with the PT series for a hydrogen atom[19,20]. Note that at $z = 1$ functions (A.4) have a singularity, $f(z)$ remaning finite at $z=1$:

$$f(z) = A\left[1 + \frac{3}{16}y\ln y + O(y)\right],$$

$$g(z) = \frac{1}{2}A\left[\frac{1}{y} - \frac{9}{16}\ln y + O(1)\right], \qquad (A.7)$$

$$h(z) = -\frac{3}{2}A\ln y + O(1).$$

where $y = 1 - z \to 0$ and $A = 2^{7/2}/3\pi = 1.2004$

Appendix B.

Rewrite eq.(6) in the form suitable for iteration at $P \to 0$:

$$\tau = f(-16 F \tau^{-4}), \quad \varepsilon_{cl}(F) = -\tau^2, \tag{B.1}$$

where f-function defined in (4). If variable $\tau = \tau(F)$ is found up to terms of order F^k, then $F\tau^{-4}$ is known up to F^{k+1}. As a result eq.(B.1), with expansion (A.4) taken into account, allows us to find the (k+1)-th coefficient of PT for $\varepsilon_{cl}(F)$. Finally,

$$\tau = 1 - 3/2\ F - 1/4\ F^2 - 39/16\ F^3 + \ldots, \tag{B.2}$$

$$\varepsilon_{cl} = -1 + 3F - 7/4\ F^2 + 33/8\ F^3 - 465/32\ F^4 + \\ + 1995/32\ F^5 - 77\ 027/256\ F^6 + \ldots - 9\ 724\ 330\ 239/32\ 768\ F^{10} + \\ + \ldots$$

and, for instance, the coefficient at F^{50} is $\approx -1.937.10^{39}$. The value $\varepsilon_{cl}(F)$ grows together with F and at $F = F_*$ vanishes, $\varepsilon_{cl}(F_*) = 0$:

$$F_* = \left[\, 1/2\ F(1/2,\ 5/2;\ 2\ ;\ 1/2)\ \right]^4 = \left(\frac{2\gamma}{9\pi}\right)^2 = 0.3834, \tag{B.3}$$

where $\gamma = \left[\Gamma(\frac{1}{4})/\Gamma(\frac{3}{4})\right]^2 = 8.753\ 757\ \ldots$ At $F \geq F_*$ eq.(6) becomes inconvenient. Putting $y = \varepsilon(\varepsilon^2 + 16F)^{-1/2}$ and using the Kummer transformation one may transform (6) into

$$\varepsilon_{cl}(F) = 4\ F^{1/2}\ y(1-y^2)^{-1/2}, \\ (1-y^2)^{1/4} \cdot F\ (1/2,\ 5/2;\ 2;(1+y)/2) = 2\ F^{1/4}, \tag{B.4}$$

which gives $\varepsilon_{cl}(F)$ parametrically $(-1 \leq y < 1)$.

Hence it is clear that the point y=0 (i.e $F=F_*(1,0)$) is not singular and $\mathcal{E}_{cl}(F)$ remains real at all F. At F close to F_*, $\mathcal{E}_{cl}$ may be expanded into series (7) and

$$\alpha_1 = \frac{\gamma^2}{27\pi} = 0.9034, \quad \alpha_2 = \frac{1}{8}\left(1-\frac{\gamma^2}{48}\right)\alpha_1 = -0.0674, \tag{B.5}$$

$$\alpha_3 = 3/32(-1 + \gamma^2/216 + \gamma^4/6912)\cdot\alpha_1 = 0.0173, \ldots$$

and γ is a constant defined at (B.3). Fast decrease of $|\alpha_k|$ with growing k accounts for approximate linearity of $\mathcal{E}_{cl}(F)$ within $0.3 < F < 0.8$, which is clearly seen from Figs.2-4.

According to symmetry relation [18]

$$E^{(n_1 n_2 m)}(\mathcal{E}) = E^{(n_2 n_1 m)}(-\mathcal{E}) \tag{B.6}$$

the function $\mathcal{E}_{cl}(F)$ at $F < 0$ corresponds to (0,n-1,0) states with $F > 0$ and $n \to \infty$. Therefore, it has singularity at F = $= -F_*(0,1) = -0.129$. Due to this, series (7) converges in the region

$$|f| < 1 + \frac{F_*(0,1)}{F_*(1,0)} = 1.339, \qquad f = \frac{F}{F_*(1,0)} - 1 \tag{B.7}$$

Consequently, $\alpha_k \sim (-)^{k+1} a^k k^\beta$ at $k \to \infty$ where $a = -1/1.399 \approx 0.715$.

Function $\gamma_{cl}(F)$ entering (6), at $F \to F_*$ has a square root

singularity:

$$\gamma_{cl}(F) = \left[(1+f)\frac{d}{df} - 1\right] \varepsilon_{cl}^{3/2} =$$

$$= a f^{1/2}\left[1 + bf + cf^2 + \cdots\right] \cdot \theta(f) \quad \text{(B.8)}$$

where

$$a = \gamma^2/2\cdot(3\pi)^{1/2} = 1.288,\ b = 31/48(1-5\cdot\gamma^2/496) =$$
$$= 0.147\ ,\ c = -0.0399,\ \ldots \quad \text{(B.9)}$$

These formulae can be used when calculating ε_{cl} , γ_{cl} at $F \approx F_*$. The accuracy of approximation is increased if the corresponding PA's $[1/1]$ is used instead of three terms of a power series.

In conclusion, let us give asymptotics of $\varepsilon_{cl}(F)$ at $F \to \infty$. In this case $y \to 1$, and taking into account that

$$F\left(\tfrac{1}{2}, \tfrac{5}{2}; 2; \tfrac{1+y}{2}\right) = \frac{8}{3\pi(1-y)} - \frac{1}{\pi}\ln(1-y) +$$
$$+ \frac{5}{\pi}\left(\ln 2 - \frac{1}{3}\right) + O\left((1-y)\ln(1-y)\right),$$

we get

$$\varepsilon_{cl}(F) = (3\pi F)^{2/3}\cdot\left[1 + c_1 F^{-1/3}\ln F + c_2 F^{-1/3} + O(F^{-2/3}\ln F)\right]$$

$$c_1 = \frac{2}{3}(3\pi)^{-4/3} \approx 0.0355, \quad \text{(B.10)}$$

$$c_2 = (3\pi)^{-4/3}\left(17\ln 2 - \frac{8}{3}\ln 3\pi + \frac{3}{2}\right) = 0.367$$

Table 2 for ε_{cl} , γ_{cl} was calculated using summation of PT series (B.2) with the help of PA's $[L/L](F)$.

For $(0,n_2,0)$ states with $n_2 = n - 1 \gg 1$ and $F \to \infty$

$$\epsilon_0(F) = -(3\pi F)^{2/3} e^{i\pi/3} \left\{ 1 + O\left(F^{-1/3} \ln F\right) \right\} \quad \text{(B.9)}$$

The corresponding formula for (0,0,n-1) states is easily obtained from eq.(13). Let $u = 1 - \tau^2$, then $\epsilon_0 = 3u^3 - 4u^2$, $u^3 - u^2 = F^2$. If we substitute $u = e^{-i\pi/3} F^{2/3} z^{1/3}$, then

$$z = 1 + \lambda z^{8/3}, \quad \epsilon_0 = 3 e^{-i\pi/3} F^{2/3} \left(z^{1/3} - \frac{4}{3} \lambda z^{2/3} \right),$$

where $\lambda = e^{i\pi/3} F^{-2/3} \to 0$ and $z \to 1$. The above equations are convenient for the application of Lagrange's formula, well-known from the theory of analytic functions. Finally, we get

$$\epsilon_0 = 3 e^{-i\pi/3} F^{2/3} \left\{ 1 - d_1 F^{-2/3} - d_2 F^{-4/3} + \cdots \right\}, \quad \text{(B.10)}$$

where $d_k = \frac{2}{3} \left[\Gamma\left(\frac{8k-6}{3}\right) \Big/ k! \, \Gamma\left(\frac{12-k}{3}\right) \right] \cdot e^{i\frac{k\pi}{3}}$, $k \geq 1$

In all the cases at hand the leading term of 1/n-expansion $\epsilon_0 \sim F^{2/3}$ at $F \to \infty$, but the structures of these expansions are different, compare eqs.(B.8),(B.9) with eq.(B.10). Note that the imaginary part of $\epsilon_0(F)$ is zero only in the case (B.8).

Notes

1) There are a few more papers dealing with calculations of the Stark shifts and widths of a hydrogen atom in strong electric field , $n^4\mathcal{E}\sim 1$. However, these calculations do not pertain to those cases (namely, $n_1 \sim n = 20\div 40$, n_2 and $m \sim 1$, $F \sim F_*$), where a comparison with experimental data is possible.

2) Here r_a is the atomic core radius; hereafter we assume that $r_a << \bar{r} \sim n^2$ for the Rydberg states.

3) For hydrogen $\mu_\ell = \delta(n_1 n_2 m) \equiv 0$. Due to spin-orbit interaction quantum defects μ_ℓ depend not only on ℓ but also on the total angular momentum j, though this dependence is not essential [10] . We assumed, in accordance with statistical weight,

$$\mu_\ell = \frac{1}{2\ell+1}\left[(\ell+1)\mu_\ell^+ + \ell\mu_\ell^-\right],$$

where $\mu_\ell^\pm = \mu_{j\ell}$ at $j = \ell \pm 1/2$.

Note also that at $n \to \infty$ and fixed n_2, m

$$\delta(n_1 n_2 m) = \frac{c}{n} + O\left(\frac{1}{n^2}\right), \quad c = \sum_\ell (2\ell+1)\mu_\ell$$

However, this asymptotics is established rather slowly, and at $n \sim 30$ an exact formula (3) must be used.

4) We introduced here a correction for the barrier penetreability according to eq.(15). As follows from the Table given below, the effect of the correction changes the position of resonances by less than 0.5 cm^{-1} which is smaller than experimental errors (the numbers belong to a hydrogen atom, $\delta = 0$, at $\mathcal{E} =$

= 16.8 kV/cm; in column I the correction is not included, while in column II it is).

$(n_1 n_2 m)$	n	$-E_r^{(n_1 n_2 m)}$, cm^{-1}	
		I	II
17, 0, 0	18	58.41	58.01
16, 0, 0	17	122.66	123.14
15, 0, 0	16	196.44	196.63
14, 1, 0	16	234.82	235.16
11, 3, 0	15	384.13	384.39
10, 4, 0	15	418.71	419.08

On the other hand, when calculating the widths $\Gamma^{(n_1 n_2 m)}$ the effect of this correction is extremely important and must be taken into account, that is the case in Table 3.

5) Experimental values $E_r^{(n_1 n_2 m)}$ have errors $2cm^{-1}$ [4,5]. Therefore, two last digits in E_{exp} (Table 3), apparently, should be neglected.

6) We have checked that eq.(10) is in agreement with experimental spectra for H[4,5] and Ne[2].

7)On the other hand, if experimental data in $E < 0$ region are treated according to eq.(8), then deviations from the curve $\varepsilon_{cl}(F)$ considerably exceed experimental errors and rapidly increase with the growth of p = 1,3, ... 9.

8) At $F \to 0$, using PS and eq.(A.7), we obtain from (22):

$$z_2 = 8(1-x)F + O(F^2),$$

$$a = \frac{n}{2\pi}\left\{\frac{2}{3F} + (1-x)\ln F - \right.$$
$$\left. - [3x + (1-x)(1+3\ln 2 - \ln(1-x))] + \cdots\right\}$$

Hence it follows that formula

$$\Gamma^{(n,n_2 0)} = \frac{1}{2\pi n^3} e^{-2\pi a} = \frac{e^{3nx}}{2\pi n^3}\left[\frac{8e}{(1-x)F}\right]^{n(1-x)} \cdot \exp\left(-\frac{2n}{3F}\right)$$

differs from exact asymptotics[15,16]

$$\Gamma^{(n,n_2 0)} \approx \frac{e^{3n}}{n^3(n_2!)^2}\left(\frac{4n}{e^3 F}\right)^{p} \exp\left(-\frac{2n}{3F}\right), \quad F \to 0$$

only in substituting $n_2!$ according to the Stirling formula (here $p = 2n_2 + 1 = n(1-x)$, $\nu_2 = (n_2 + 1/2)n^{-1} = (1-x)/2$).

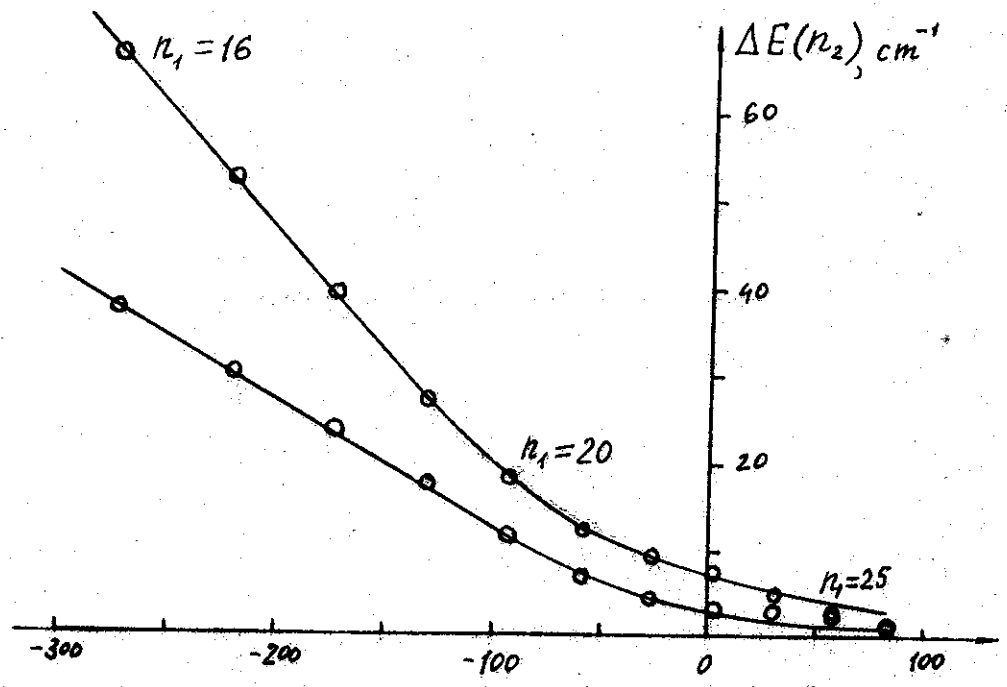

Fig.1. a) Energy differences $\Delta E(n_2) = E_r^{(n_1 n_2 0)} - E_r^{(n_1 00)}$ for states with $n_2 = 1$ (lower curve) and $n_2 = 2$ (upper curve). The values of $E \equiv E_r^{(n_1 00)}$ are plotted along abscissa axis.

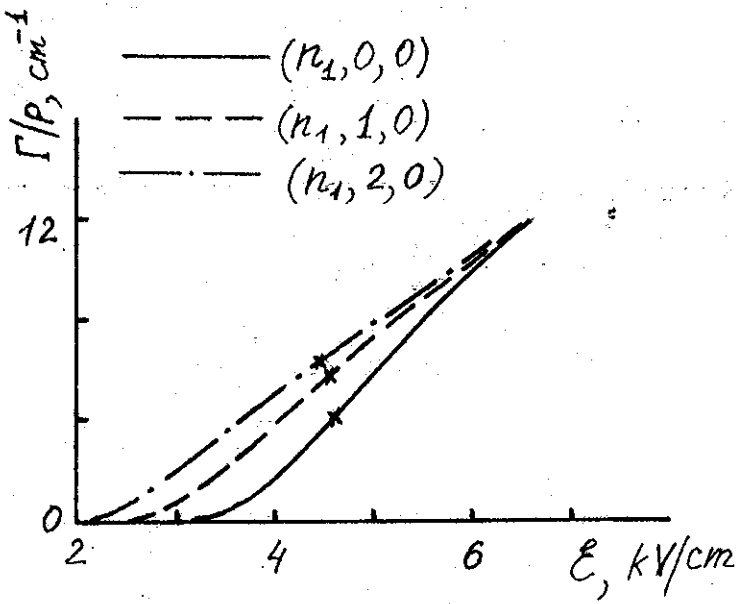

Fig.1 b) The ratio $\Gamma^{(n_1, n_2, 0)}(\mathcal{E})/p$ for $n_1 = 25$, $n_2 = 0, 1$ and 2 ($P = 2n_2 + 1$). The intersection of the ionization limit $E = 0$ is marked by cross.

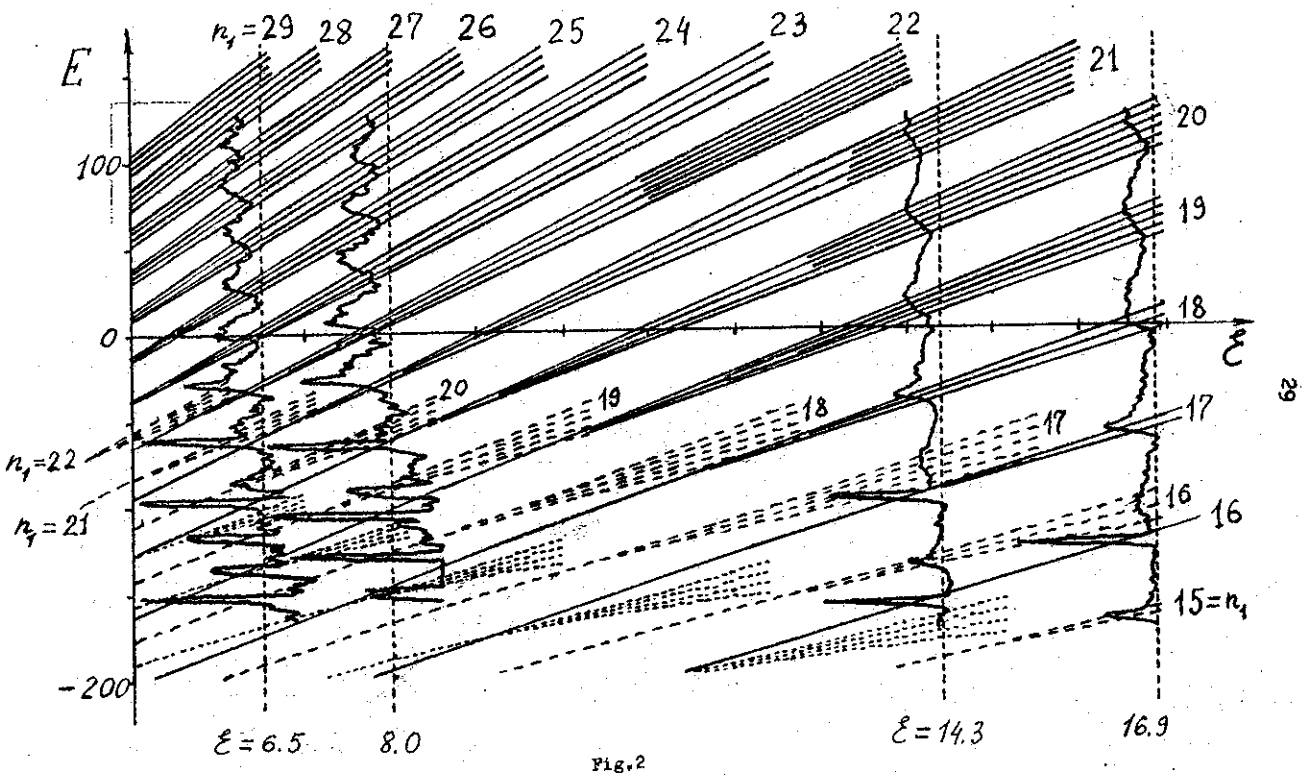
E
100
0
-200
n_1=29
28
27
26
25
24
23
22
21
20
19
18
17
16
n_1=15
n_1=22
n_1=21
ε
ε = 6.5
8.0
ε = 14.3
16.9

Fig.2

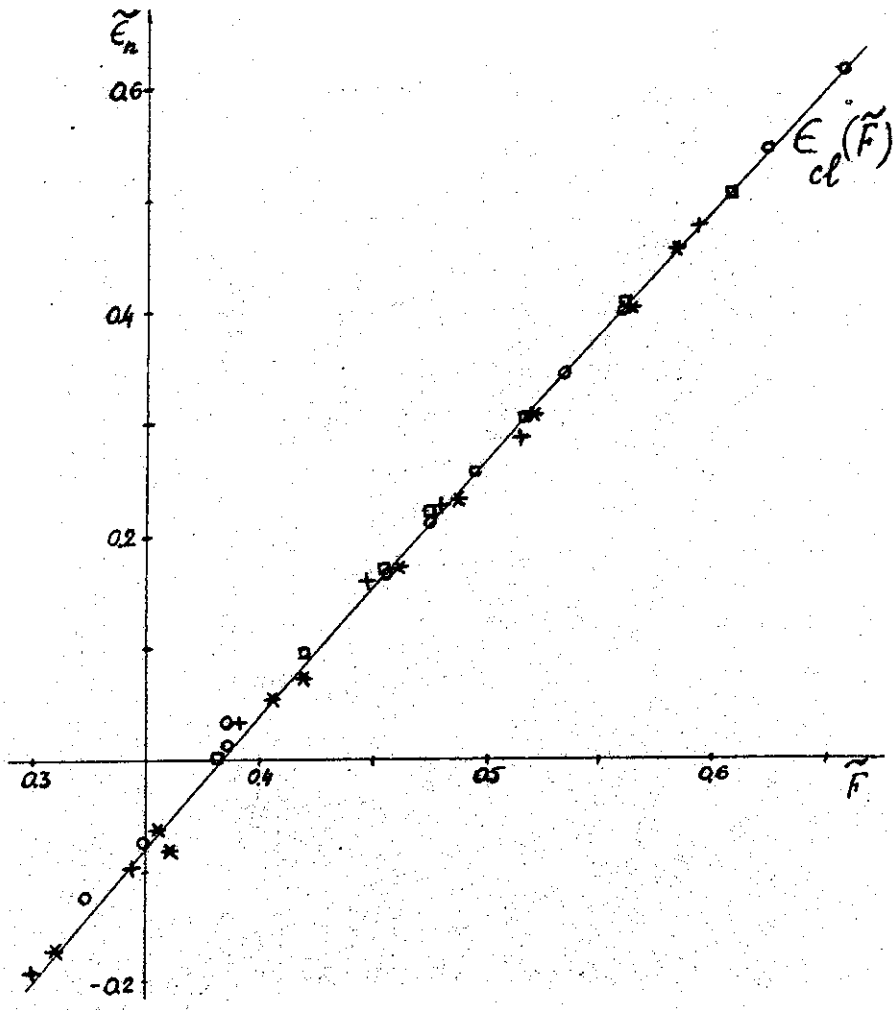

Fig.3. Scaling in $B > 0$ region. The notations of experimental points are given in the text.

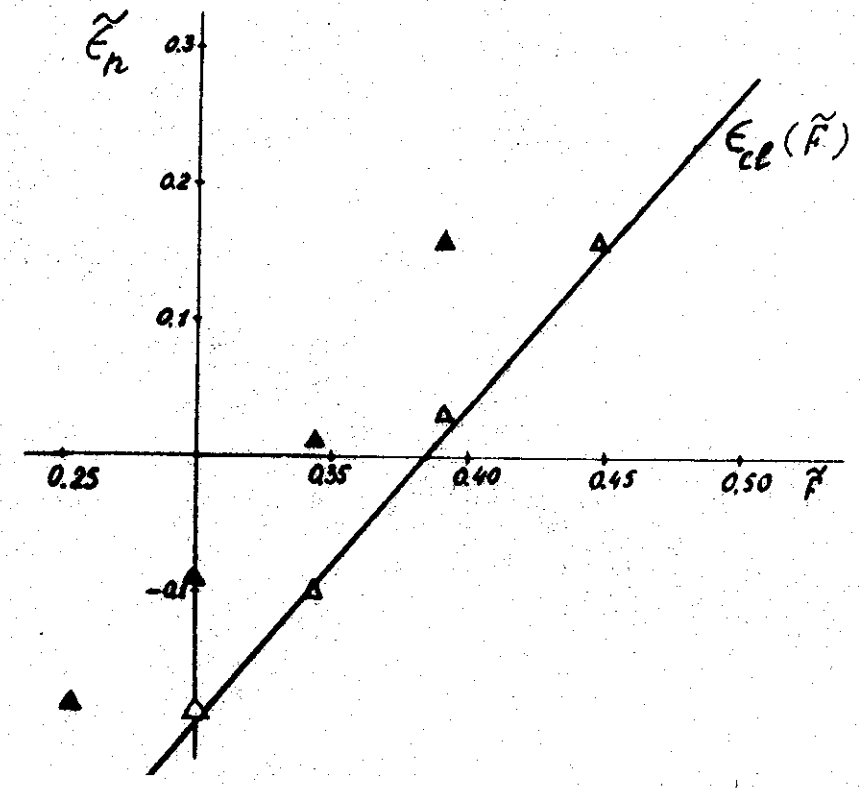

Fig.3a. Processing of experimental spectrum for Rb: △ - with the change n → n+1, ▲ - without it. Solid curve corresponds to $\epsilon_{cl}(\tilde{F})$.

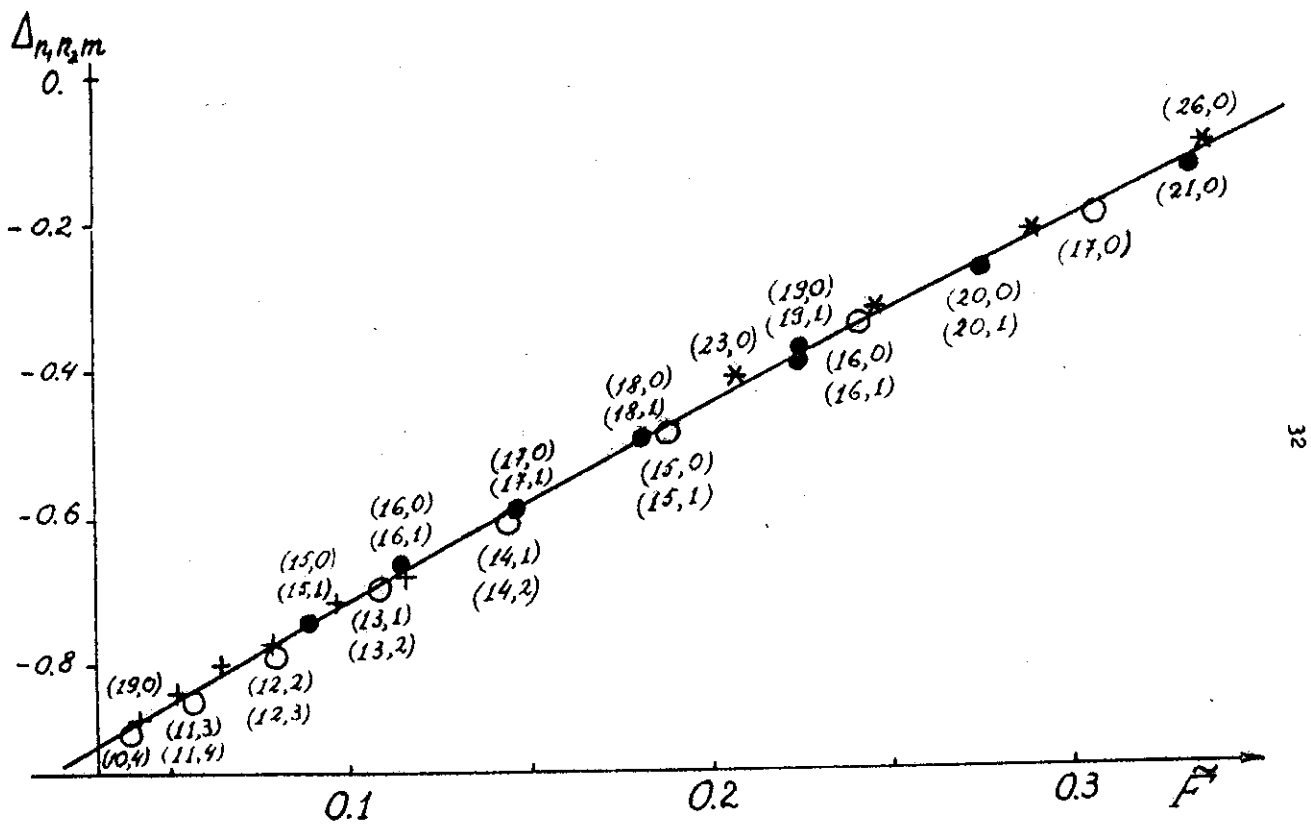

Fig.4. Scaling in E < 0 region.

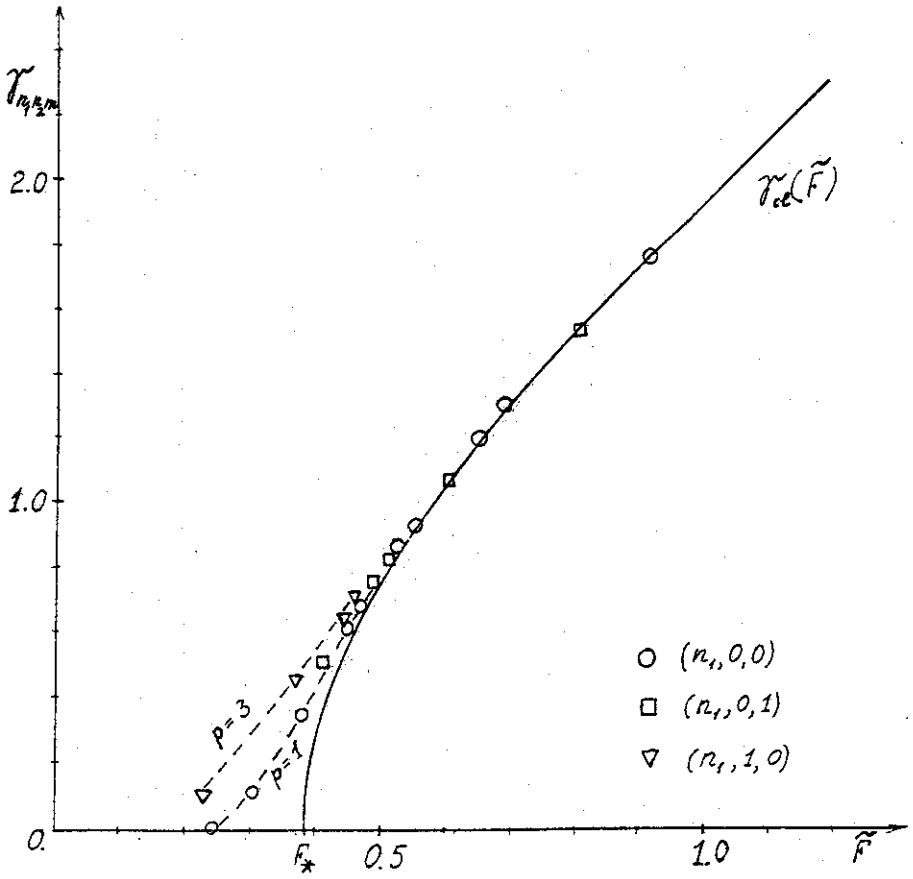

Fig.5. Scaling (8) for the widths of the Stark resonances (a hydrogen atom, $\mathcal{E}$ = 6.5 and 8.0 kV/cm [4]). The values $\gamma_{n_1n_2m} = p^{-1}\tilde{n}^3 \Gamma^{(n_1n_2m)}(\mathcal{E})$ are plotted along the ordinate axis ($\tilde{n} = n_1 + \frac{m+1}{2} = n - p/2$, $\Gamma^{(n_1n_2m)}(\mathcal{E})$ is the width of (n_1n_2m) state in atomic units).

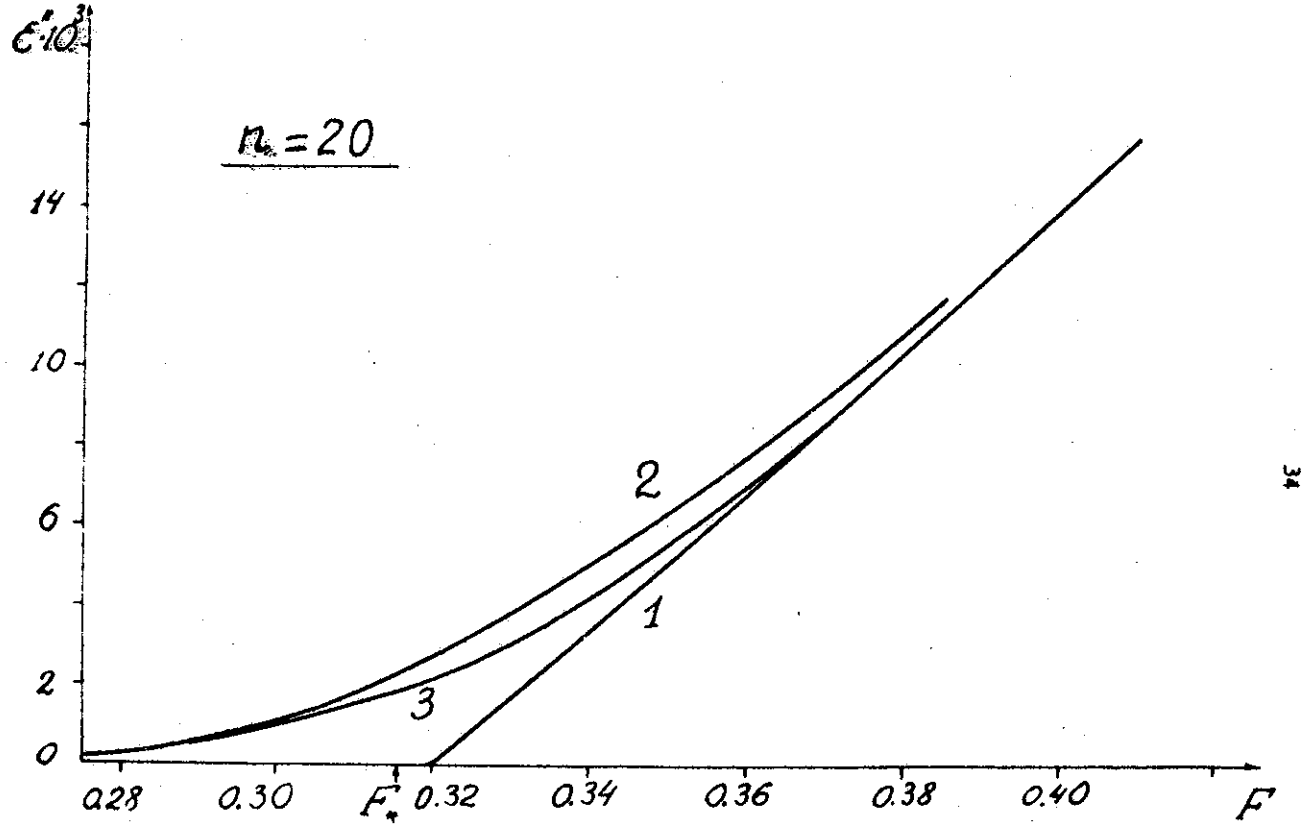

Fig.6. The barrier penetrability effect on ε_n'' for (n-1 ,0,0) states (n = 20, $F_* = 0.315$).

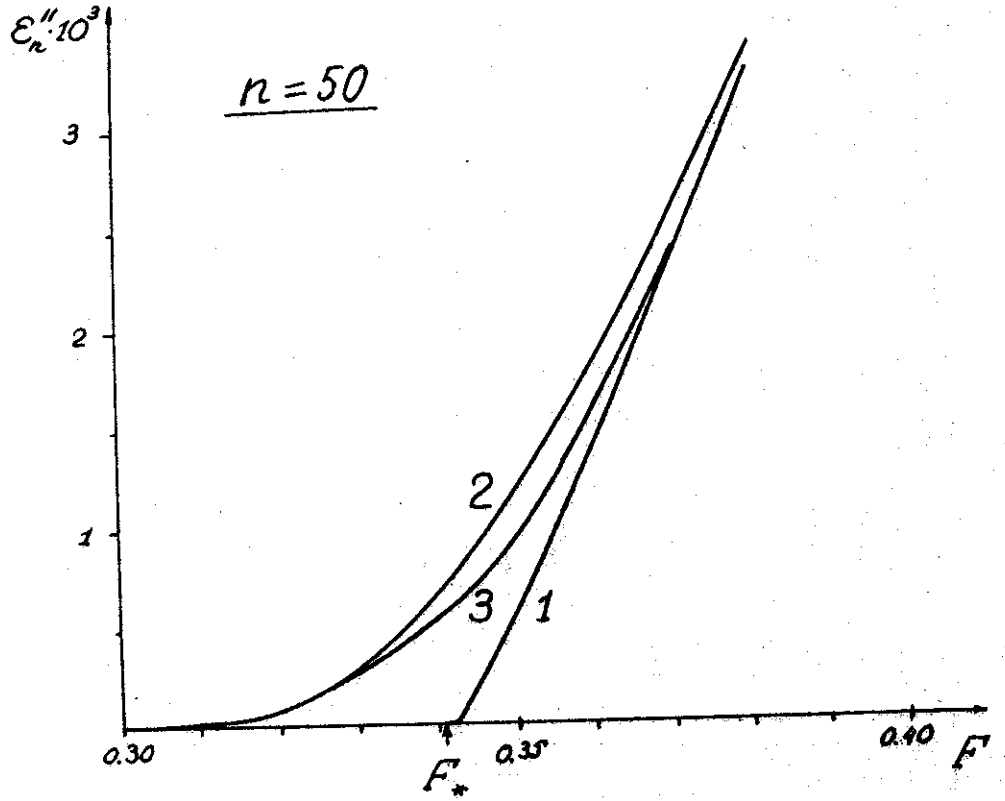

Fig.7. The same as in the preceding figure, for n = 50 (F_* = = 0.341).

Table 1

The quantum defects $\delta(n, n_2 m)$ in parabolic basis for rubidium, Z=37.

n	$(n_1,0,0)$	$(n_1,1,0)$	$(n_1,2,0)$	$(n_1,0,1)$	$(n_1,0,2)$
18	0.840	0.594	0.435	0.317	1.25(-2)
20	0.768	0.561	0.421	0.275	9.29(-3)
25	0.633	0.491	0.386	0.204	4.91(-3)
30	0.538	0.435	0.355	0.161	2.90(-3)
35	0.468	0.390	0.327	0.131	1.86(-3)
40	0.414	0.353	0.302	0.111	1.26(-3)
50	0.336	0.296	0.261	0.084	-

Footnote. Hereafter the order of magnitude is given in brackets: 1.25(-2) = 0.0125, etc.

Table 2

Fanctions $\varepsilon_{cl}(F)$ and $\gamma_{cl}(F)$.

F	$-\varepsilon_{cl}$	F	ε_{cl}	γ_{cl}	F	ε_{cl}	γ_{cl}
0	I.0000	0.39	0.0I55	0.I693	0.54	0.3587	0.8678
0.05	0.8539	0.40	0.0390	0. 2696	0.55	0.38I0	0.8977
0.I0	0.7I44	0.4I	0.0623	0.3426	0.56	0.4032	0.9270
0.I5	0.5800	0.42	0.0856	0.4033	0.58	0.4475	0.9837
0.20	0.4499	0.43	0.I088	0.4567	0.60	0.49I4	I.0384
0.25	0.3233	0.44	0.I3I9	0.505I	0.65	0.6003	I.I675
0.30	0.I999	0.45	0.I550	0.5498	0.70	0.7076	I.2884
0.3I	0.I756	0.46	0.I779	0.59I7	0.75	0.8I35	I.4030
0.32	0.I6I3	0.47	0.2008	0.63I2	0.80	0.9I82	I.5I26
0.33	0.I272	0.48	0.2236	0.6689	0.85	I.02I6	I.6I80
0.34	0.I032	0.49	0.2463	0.7050	0.90	I.I239	I.7200
0.35	0.0792	0.50	0.2689	0.7396	0.95	I.225I	I.8I89
0.36	0.0554	0.5I	0.29I5	0.773I	I.00	I.3252	I.9I53
0.37	0.03I7	0.52	0.3I40	0.8056	I.I0	I.5226	2.I0I2
0.38	0.0080	0.53	0.3364	0.837I	I.20	I.7I63	2.2797

Table 3

Energies and Halfwidths of the Stark resonsnces with m=0 in a hydrogen atom, $\mathcal{E}$ = 16.8 kv/cm

(n_1,n_2)	n	$-E^{(n_1,n_2\rho),cm^{-1}}$ HPA	1/n	exp.[5]	$\Gamma/2,cm^{-1}$ HPA	1/n	exp.[5]
I7,0	I8	58.2	58.0	60.72	2.3	2.2I	2.5
I6,I	I8	I06.6	I06.6	I03.75	8.9	8.8	9
I6,0	I7	I23.5	I23.I	I26.46	0.I8	0.I53	0.I4
I5,I	I7	I67.7	I67.5	I67.87	I.9	I.84	2.I
I5,0	I6	I96.7	I96.6	I98.54	$<I0^{-2}$	$7\cdot I0^{-4}$	$I,I\cdot I0^{-4}$
I4,2	I7	2II.6	2II.5	2I0.09	5.7	5.64	6.6
I4,I	I6	235.3	235.2	238.I2	0.0I2	0.020	0.0I6
I3,2	I6	274.3	274.2	275.8I	0.28	0.275	0.23
I3,I	I5	3I5.2	3I5.I	3I4.8I	$<3\cdot I0^{-3}$	$I.9\cdot I0^{-4}$	-
I2,3	I6	3I3.8	3I3.7	3I4.8I	I.3	I.29	I.6,2.5
I2,2	I5	349.8	349.8	35I.42	$<I0^{-3}$	$\sim I0^{-4}$	$5\cdot I0^{-5}$
II,4	I6	353.2	353.2	35I.42	3.3	3.29	3.0
II,3	I5	384.4	384.4	386.35	0.002	$I.9\cdot I0^{-3}$	$I.8\cdot I0^{-3}$
I0,4	I5	4I9.2	4I9.I	4I9.23	0.03	0.02	0.032

Table 3

(n_1,n_2)	n	$-E^{(n_1,n_2,0)}$, cm^{-1} HPA	1/n	exp.[5]	$\Gamma/2$, cm^{-1} HPA	1/n	exp.[5]
0,I3	I4	78I.8	78I.9	78I.64	0.57	0.570	0.62
I,I2	I4	750.9	750.9	75I.7	0.27	0.268	0.25
2,II	I4	720.0	720.0	72I.0	0.II	0.I05	0.II
3,I0	I4	689.I	689.I	689.I	0.033	0.034	0.04
5,8	I4	627.3	627.3	629.0	-	$I.9 \cdot I0^{-3}$	0.002
6,7	I4	596.3	596.3	597.7	0.003	-	0.003
7,6	I4	565.2	565.2	566.0	$< I0^{-4}$	$4 \cdot I0^{-5}$	$I.5 \cdot I0^{-5}$
6,8	I5	558.8	558.8	566.0	2.3	2.30	2.I,3.2
8,6	I5	488.9	488.9	490.92	0.44	0.445	0.38
9,5	I5	453.9	453.9	455.5	0.II	0.II8	0.I3

Table 4

n	F_n	n	F_n	n	F_n
I0	0.2895	23	0.3200	35	0.3323
I5	0.3054	24	0.32I4	40	0.3358
I7	0.3099	25	0.3226	50	0.34I2
I8	0.3II9	26	0.3238	60	0.3452
I9	0.3I38	27	0.3250	70	0.3484
20	0.3I55	28	0.326I	80	0.3509
2I	0.3I7I	29	0.327I	90	0.3530
22	0.3I86	30	0.328I	I00	0.3548
				∞	0.3834

Footnote. Here we give the values of the classical ionization thereshold F_n for the states with m=0 ($\nu_2 = 1-\nu_1 = 1/2n$, $x=1-n^{-2}$).

Table 5

F	n = 20		n = 50	
	1/n	$1/n^2$	1/n	$1/n^2$
0.20	0.4828	0.4831	0.46304	0.46309
	0.4830	0.4831	0.46307	0.46309
0.25	0.3663	0.3669	0.34048	0.34057
	0.3668	0.3670	0.34054	0.34057
0.30	0.2549	0.2570	0.22169	0.22192
	0.2562	0.2566	0.22186	0.22193
0.35	0.1508	0.1574	0.10793	0.10935
	0.1490	0.1488	0.10768	0.10775
0.37	0.1084	0.1169	0.06333	0.06586
	0.1063	0.1058	0.06263	0.06252
0.38	0.0870	0.0962	0.0408	0.0436
	0.0849	0.0843	0.0401	0.0399
0.39	0.0654	0.0751	0.0181	0.0210
	0.0635	0.0628	0.0176	0.0174
0.40	0.0437	0.0537	-	-
	0.0421	0.0413	-	-

Footnote. We give the values $-\epsilon'_n$ for (n-1,0,0) states, calculated in 1/n- and $1/n^2$-approximations. The first line - without the barrier penetreability, the second - including it.

References

1. Freeman R.R., Economou N.P.// Phys.Rev.,1979,v.A20,p.2356.
2. Luk T.S., Di Mauro L., Bergman T., Metcalf H.// Phys.Rev.Lett. 1981,v.47,p.83.
3. Sandner W., Safinya K.A., Gallagher T.F.// Phys.Rev.A.,1981, v.23,p.2448.
4. Glab W.L., Ng K., Yao D., Nayfeh M.N.,//Phys.Rev.A,1985,v.31, p.3677.
5. Ng K., Yao D., Nayfeh M.N.// Phys.Rev.A,1987,v.35,p.2508.
6. Kolosov V.V.// Pis'ma v ZhETP,1986,v.44,p.457.
7. Weinberg V.M.,Mur V.D.,Popov V.S.,Sergeev A.V.// Pis'ma v ZhETP,1987,v.46,p.178.
8. Bekenstein J.D., Krieger J.B.// Phys.Rev.,1969,v.188,p.130.
9. Pock V.A.// Zeits.Physik,1935,v.98,p.145.
10. Zimmerman M.L. et al.// Phys.Rev.A,1979,v.20,p.2251.
11. Weinberg V.M., Mur V.D., Popov V.S., Sergeev A.V.// Pis'ma v. ZhETP,1986,v.44,p.9; ZhETF,1987,v.93,p.450.
12. Popov V.S., Mur V.D., Shcheblykin A.V., Weinberg V.M.// Phys.Lett.A.,1987,v.124,p.77.
13. Weinberg V.M., Mur V.D., Popov V.S. et al.// Theor.Mat.Fiz., 1988,v.74,p.399.
14. Popov V.S., Weinberg V.M., Mur.V.D.// Pis'ma v ZhETF,1985, v.41,p.439; Yad.Fiz.,1986,v.44,p.1103.
15. Kadomtsev M.B., Smirnov B.M.// ZhETF,1981,v.80,p.1715.
16. Drukarev G.F.// ZhETF,1978,v.75,p.437.
17. Slavyanov S.Yu.// Problemi Mat.Fiziki,1970,v.4,p.125.
18. Yamabe T., Tachibana A.// Phys.Rev.,1977,v.16,p.877.

19. Silverstone H.J.// Phys.Rev.A,1978,v.18,p.1853.

20. Alliluev S.P., Eletsky V.L., Popov V.S.// Phys.Lett.A., 1979,v.73,p.103; 1980,v.78,p.43.

В.С.Попов и др.
Скейлинг для эффекта Штарка в ридберговских атомах.
Работа поступила в ОНТИ 10.06.88

Подписано к печати 29.06.88 Т15734 Формат 60x90 1/16
Офсетн.печ. Усл.-печ.л.2,75. Уч.-изд.л.1,6. Тираж 290 экз.
Заказ 173 Индекс 3624 Цена 24 коп.

Отпечатано в ИТЭФ, 117259, Москва, Б.Черемушкинская, 25

ИНДЕКС 3624

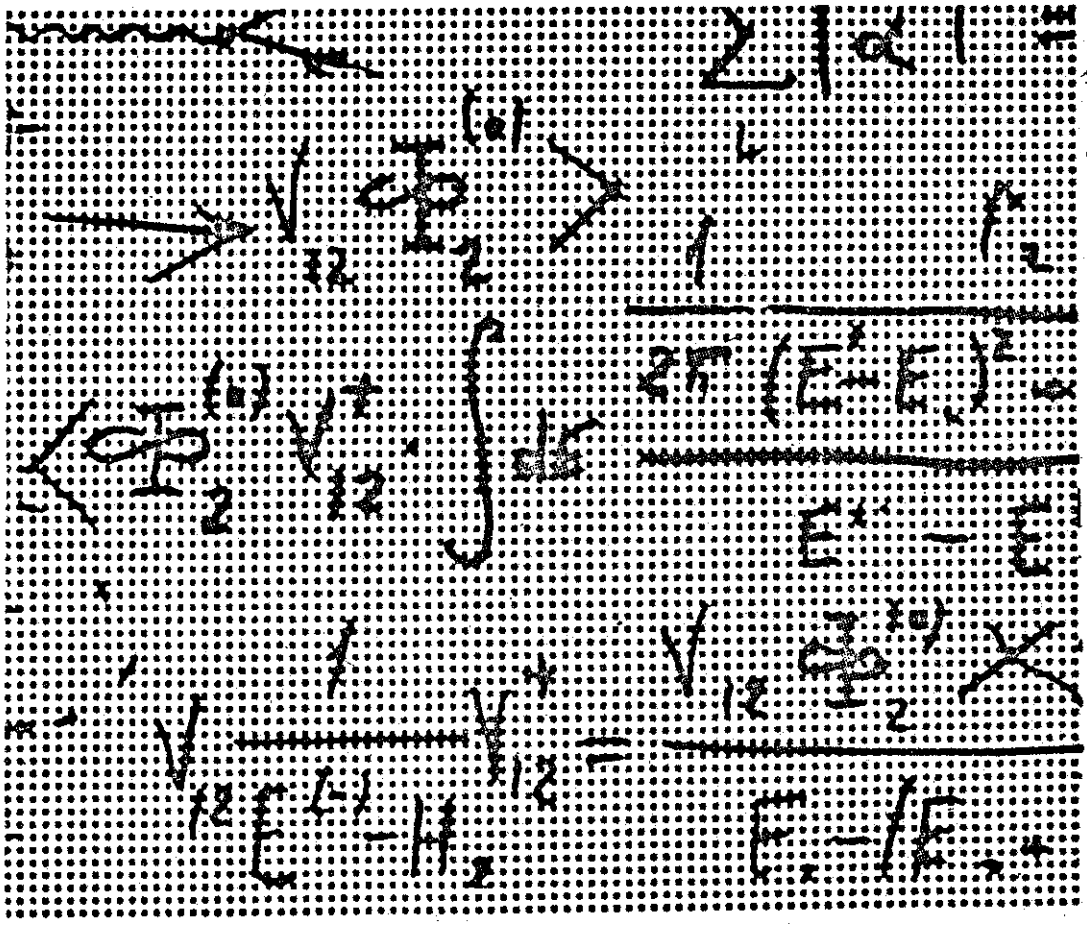

М.,Препринт ИТЭФ, 1988, № 173, с.1-44